International Journal of GEOMATE, May, 2024 Vol.26, Issue 117, pp.87-99
ISSN: 2186-2982 (P), 2186-2990 (O), Japan, DOI: https://doi.org/10.21660/2024.117.g13272
Geotechnique, Construction Materials and Environment

BEARING CAPACITY ESTIMATION OF STRIP FOOTING ON TWO-LAYERED *c*-ϕ SOILS BASED ON THE RIGID PLASTIC FINITE ELEMENT METHOD

* Hamidou Hamadoum Tamboura [1], Koichi Isobe [2]

[1] Scientific Research Section, Construction Solutions Development Department, GIKEN LTD., Kochi, Japan;
[2] Laboratory of Analytical Geomechanics, Division of Civil Engineering, Graduate School of Engineering, Hokkaido University, Japan

*Corresponding Author, Received: 14 June 2023, Revised: 17 Jan. 2024, Accepted: 18 Jan. 2024

ABSTRACT: This study investigates the bearing capacity of a strip footing on two-layered *c*-ϕ soils by considering layer factors estimated using an in-house FEM code, namely, the rigid-plastic finite element method. The influences of the following ratios on the bearing capacity factors were investigated: the ratio of the tangent of the angle of friction of the bottom layer to that of the top layer; the ratio of the cohesion of the bottom layer to that of the top layer; the ratio of the unit weight of the bottom layer to that of the top layer; and the ratios of the embedment of the footing and the thickness of the top layer to the footing width. Based on the influences of those ratios, layer factors are determined. Several types of failure mechanics were found and the conditions of occurrence of each failure type are summarized in a chart. In addition, a new approach for estimating the bearing capacity of a strip footing on two-layered *c*-ϕ soils is proposed. A comparison with available methods in the literature has confirmed the reliability of the proposed method, showing the application limitation of the past research.

Keywords: Strip Footing, Bearing Capacity, Bearing Capacity Factors, c-ϕ soil, Layered Ground, FEM

1. INTRODUCTION

Numerous researchers have contributed to the exploration of bearing capacity in footings on stratified soil.

Many researchers focused on the bearing capacity of footing on dense sand over clay. [1] focused on dense sand over clay, analyzing various failure modes and conducting model tests on circular and strip footings. [2] conducted physical model tests for sand over clay, observing shear plane inclination in the sand layer. [3] studied footings on a dense sand layer over soft clay, presenting results through design charts. [4] examined elastoplastic behavior in footings on soils with varying strengths using finite elements. [5] reported measurements of strip footings on sand over clay, covering a narrow range of sand and clay properties. [6] analyzed strip footings on a two-layer foundation, considering the kinematic approach. [7] investigated plane-strain footings on layered soils, emphasizing the influence of clay shear strength. [8] proposed methods for calculating bearing capacities, considering limit equilibrium forces. [9] obtained plasticity solutions for strip footings on a sand layer over clay. [10] utilized a multi-block upper-bound method for two-layer foundation soils. [11] employed the limit analysis method with a multi-rigid-block upper-bound approach to assess foundations over two-layered soils. [12] addressed undrained bearing capacity estimation for a rigid strip footing on a sand layer overlying clay, utilizing finite element limit analysis and the upper and lower bounds of plasticity theorems.

[13] pioneered the analysis of footings on layered soils with varying cohesion, particularly in two-layer cohesive subsoils, establishing bearing capacity coefficients. [14] delved into the ultimate bearing capacity of footings on two-layered subsoils, considering scenarios of dense over weak and loose over firm layers. [15] explored the ultimate bearing capacity of strip footings on cohesive soil with anisotropic undrained cohesion varying linearly with depth in each layer. [16] investigated bearing capacity in layered clay through model tests with circular and strip footings. [17], along with [18] numerically and experimentally analyzed circular footings on layered cohesive soils, considering stress-deformation and bearing capacity. [19] applied numerical limit analysis to assess the undrained bearing capacity of a rigid surface footing on a two-layer clay deposit. [20] employed Finite Element Limit Analysis (FELA) to investigate the undrained bearing capacity of strip footings in two-layered clays, including scenarios with voids.

The bearing capacity of shallow foundations on layered sand strata has been extensively explored by various researchers. [21] conducted a numerical investigation on the ultimate bearing capacity of a ring footing on loose sand overlying a dense sand deposit. [22] developed a theory for the ultimate bearing capacity of footings on subsoil with a strong sand layer overlying a weak sand deposit. [23]

extended the classical equation of bearing capacity for footings on homogeneous sand to address scenarios with weaker upper layers in layered sands, providing corresponding design charts. [24] experimentally estimated the bearing capacity of eccentrically loaded continuous foundations on layered sand. [25] investigated the ultimate bearing capacity of shallow foundations subjected to axial vertical loads on soil consisting of two layers, considering strong cohesionless soil overlying a weak deposit. [26] estimated the bearing capacity of dense sand overlying loose sand, considering the influence of geogrid inclusion. [27] utilized the finite-difference code (FLAC) to study the bearing capacity of isolated footing and interactions with other footings on sands. [28] estimated the bearing capacity of strip and circular footings, incorporating a dense sand layer over loose sand strata using lower and upper-bound finite element limit analysis. [29] investigated the bearing capacity of strip footings on a thin layer of dense sand overlying a weaker sand layer. Utilizing the Finite Element Limit Analysis method, they calculated the collapse load and identified the geometry of the failure mechanism.

In the realm of comparison studies focusing on shallow foundations in two-layered c-ϕ soils, there has been relatively limited attention. [30] introduced a method for estimating the bearing capacity of footings on two-layered soils with varying cohesion, friction, and unit weight, employing the second theorem of Drucker and Prager (kinematical consideration). They provided bearing capacity charts by varying cohesion in layers while maintaining the same friction angle and unit weight. [31] conducted a study to determine the ultimate bearing capacity of footings in a two-layered c-ϕ soil system. They proposed empirical equations to determine the average value of cohesion, the average value of the angle of internal friction, and the equivalent significant depth for a layered soil system. Based on these strength parameters, they presented a simplified bearing capacity theory for shallow foundations in c-ϕ soils, grounded in the Terzaghi theory. [32] developed an approach to address flat punch indentation into the Mohr-Coulomb layered half-space, employing the kinematical approach of limit analysis. They presented a kinematically admissible plane-strain failure mechanism for a typical two-layer system. [33] investigated the bearing capacity of an embedded strip footing supported by two-layer c-ϕ soils using three soils with specific strength parameters in an elastoplastic finite-element computer program. They developed a semiempirical equation for determining the ultimate bearing capacity based on the analysis results. [34] proposed a formula for calculating the bearing capacity of two-layered soils, considering the location of the central wedge on the top layer and extending to the bottom layer. [34] suggests that the depth of the central wedge of general failure is the critical thickness of the top soil layer. The formula proposed by [34] shares similarities with that of [31]. For a comprehensive overview of these studies on two-layered c-ϕ soils, refer to Table 1, where B is the footing width, H is the thickness of the top layer, H_2 is the thickness of the part of the bottom layer contributing to the bearing capacity, q is the overburden pressure, c_1 is the cohesion of soil in the top layer, c_2 is the cohesion of soil in the bottom layer, ϕ_1 is the angle of friction of soil in the top layer, ϕ_2 is the angle of friction of soil in the bottom layer, and γ_1 is the unit weight of soil in the top layer.

In contrast to many empirical studies that rely on average strength for two soil layers, this study adopts a more nuanced approach. Utilizing Rigid Plastic Finite Element Method (FEM) analysis, the study delves into estimating the bearing capacity of two-layered c-ϕ soils by assigning distinct shear strengths to each soil layer. Layer factors, denoted as L_c, L_q and, L_γ, are introduced to account for the influence of the bottom layer on the bearing capacity of the top layer. Essentially, the study attempts to establish a novel methodology for determining strip footing bearing capacity on two-layered c-ϕ soils. Furthermore, the study elucidates the conditions under which different failure types occur. This approach seeks to provide a more accurate and detailed understanding of the bearing capacity in such layered soil systems.

2. RESEARCH SIGNIFICANCE

The results of this study will provide a geotechnical basis for making wise engineering decisions during the foundation of buildings and structures. The knowledge gained will help to save lives and avoid economic losses. Understanding the failure mechanism of shallow foundations in two-layered c-ϕ soils will address technical concerns about these types of foundations.

3. CONSTITUTIVE EQUATIONS FOR RIGID PLASTIC FINITE ELEMENT METHOD

The rigid-plastic finite element method (RPFEM) was developed for geotechnical engineering by [35] and [36]. The method is effective in the calculation of the ultimate bearing capacity of shallow foundations in multi-layered ground.

In this study, the in-house RPFEM code developed and updated by [37] and [38] is used to estimate the bearing capacity of a strip footing on two-layered c-ϕ soils. The rigid plastic constitutive equation for the Drucker-Prager yield function Eq. (1) is employed in the code in plane-strain conditions considering the associative flow rule.

$$f(\boldsymbol{\sigma}) = \alpha I_1 + \sqrt{J_2} - \kappa = 0 \tag{1}$$

where I_1 = tr ($\boldsymbol{\sigma}$) is the first invariant, $J_2 = \frac{1}{2}\mathbf{s}:\mathbf{s}$, $\boldsymbol{\alpha}$ and $\boldsymbol{\kappa}$ are soil parameters expressed for plane strain conditions as follows:

Table 1 Summary of existing theories on ultimate bearing capacity of two-layered c-ϕ

Reference	Formula	Specifications
Satyanarayana and Garg (1980) [31]	$q_{\text{ult}} = c_{\text{av}}N_{\text{c}} + qN_{\text{q}} + 0.5\gamma_1 BN_{\gamma}$	$c_{\text{av}} = \frac{Hc_1+H_2c_2}{H+H_2}$; $\phi_{\text{av}} = \tan^{-1}\left(\frac{H\tan\phi_1+H_2\tan\phi_2}{H+H_2}\right)$; $H_2 = (2B-H)(\frac{c_1+tan\,\phi_1}{c_2+tan\,\phi_2})$; N_c, N_q and N_γ are bearing capacity factors based on ϕ_{av}. c_{av} and ϕ_{av} are average cohesion and average frictional angle respectively.
Azam and Wang (1991) [33]	$q_{\text{ult}} = q_t + (q_b - q_t)\,[1 - m(H/B)]^2$	q_t = ultimate bearing capacity of the footing supported by an infinitely thick top-layer soil; q_b = ultimate bearing capacity of the footing supported by an infinitely thick bottom-layer soil; m = empirical parameter, which is 0.17-0.23 for two layers of clay and 0.30 for a sand-clay layer combination; $H/B \leq 6$ for clay-clay layers and $H/B \leq 3.5$ for sand-clay layers
Bowles (1996) [34]	$q_{\text{ult}} = c_{\text{m}}N_{\text{c}} + qN_{\text{q}} + 0.5\gamma_1 BN_{\gamma}$	$d = \frac{B}{2}\tan(45+\frac{\phi_1}{2})$; if $d > H$ then $\phi_m = (\frac{H\phi_1+(d-H)\phi_2}{d})$; $c_m = (\frac{Hc_1+(d-H)c_2}{d})$; N_c, N_q and N_γ are bearing capacity factors based on ϕ_m. c_m and ϕ_m are average cohesion and average frictional angle respectively.

$$\alpha = \frac{\tan\phi}{\sqrt{9+12\tan^2\phi}},\ \kappa = \frac{3c}{\sqrt{9+12\tan^2\phi}} \quad (2)$$

where c is cohesion, ϕ is shear resistance angle.
The rigid plastic constitutive equation is expressed as follows:

$$\boldsymbol{\sigma} = \frac{\kappa}{\sqrt{3\alpha^2+\frac{1}{2}}}\frac{\dot{\boldsymbol{\varepsilon}}}{\dot{e}} + P(\dot{\varepsilon}_v - \eta\dot{e})\left(\mathbf{I} - \eta\frac{\dot{\boldsymbol{\varepsilon}}}{\dot{e}}\right) \quad (3)$$

where $\dot{\boldsymbol{\varepsilon}}_v$ = volumetric strain rate, $\dot{\boldsymbol{\varepsilon}}$ = Strain rate, $\dot{\boldsymbol{e}}$ = norm of the strain rate. $\mathbf{I}$ express the unit stress tensors. η = a coefficient related to the dilation characteristics and P = penalty constant.

4. FINITE ELEMENT MESH AND ANALYSES PARAMETERS

Fig. 1 shows a schematic view of the analysis object and an illustration of the finite element mesh used and the boundary conditions. The dimensions of the model geometry are selected to avoid the undesirable effects of the boundaries. The left and right sides of the domain were pinned, enabling movement in the vertical direction while restricting movement in the horizontal direction. The bottom boundary of the domain was fixed, restricting any movement. An increasing load in a downward direction was applied on the footing.

The footing is lying on two soil layers: a topsoil layer with a thickness H, a cohesion c_1, a shear resistance angle ϕ_1, and a unit weight γ_1; and a bottom soil layer with a cohesion c_2, a shear resistance angle ϕ_2, and a unit weight γ_2. With a unit weight γ, the soil above the footing base was not modeled and was only represented by a surcharge γD_f, where D_f is the footing embedment.

The analysis parameters are as follows:
1) The ratio of the thickness of the top layer H to the footing width B (H/B). H/B was varied from 0 to 6.
2) The ratio of the tangent of the shear resistance angle of the bottom layer to that of the top layer (r_ϕ = tan (ϕ_2) / tan (ϕ_1)). The ratio r_ϕ was varied from 0.4 to 2.5. The values ϕ_2 = 20° and ϕ_2 = 42° were chosen for the case of $r_\phi \leq 1$ and the case of $r_\phi \geq 1$, respectively.
3) The ratio of the cohesion of the bottom and top layers ($r_c = c_2 / c_1$). r_c was varied from 0.25 to 4.
4) The ratio of the unit weight of the bottom layer to that of the top layer ($r_\gamma = \gamma_2 / \gamma_1$). The ratio r_γ was varied from 0.64 to 1.57.
5) The ratio of the embedment D_f to the footing width B (D_f/B). For a shallow foundation, $D_f \leq$ B, [39]. Hence, a range of D_f/B = 1 to 0.25 was used.

5. DEFINITION OF THE LAYER FACTORS

Fig. 2 explains the method used to determine the layer factors L_c, L_q, and L_γ. While for a uniform soil the bearing capacity factors are N_c, N_q, and N_g, for the layered system of two-layered c-ϕ soils (Fig. 1), the bearing capacity factors are referred to as N_c*, N_q*, and N_g*. Fig. 2 explains how N_c*, N_q*, and N_g* are calculated.

The layer factors are then obtained as ratios of bearing capacity factors of the layered system to that of a uniform ground made of the topsoil layer,

$L_i = N_i^*/N_i$, with i = c, q, γ (i.e. $L_c = N_c^*/N_c$, $L_q = N_q^*/N_q$ and $L_g = N_g^*/N_g$).

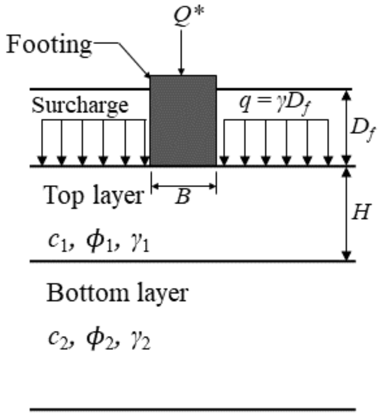

(a) Schematic view (problem definition)

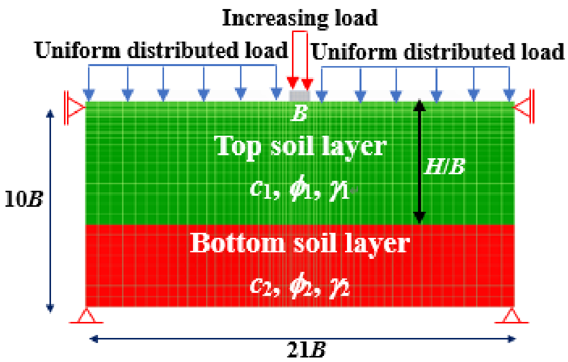

(b) FE mesh

Fig. 1 Problem Schematic view and FE mesh

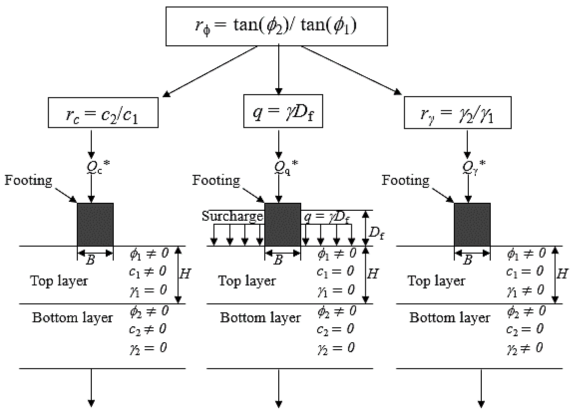

$q_c^* = c_1 N_c^*$ $\quad$ $q_q^* = q N_q^*$ $\quad$ $q_\gamma^* = 0.5\gamma_1 B N_\gamma^*$

$N_c^* = q_c^* / c_1$ $\quad$ $N_q^* = q_q^* / q$ $\quad$ $N_\gamma^* = q_\gamma^* / 0.5\gamma_1 B$

$L_c = N_c^*/ N_c$ $\quad$ $L_q = N_q^*/ N_q$ $\quad$ $L_\gamma = N_\gamma^*/ N_\gamma$

$L_c = f(H/B, r_\phi, r_c)$, $L_q = f(H/B, r_\phi, D_f)$, $L_\gamma = f(H/B, r_\phi, r_\gamma)$

Fig. 2 Definition of the layer factors L_c, L_q, and L_γ

6. INFLUENCE OF H/B ON THE LAYER FACTORS (DESIGN CHARTS PART I)

As depicted in the diagram in Fig .2, the thickness of the topsoil layer (H/B) affects all the layer factors. For the investigation of the influence of the normalized thickness of the topsoil layer (H/B) on the layer factors, $r_c = 1$, $D_f/B = 1$, and $r_\gamma = 1$ (with $c_1 = c_2 = 25$ kPa and $\gamma = \gamma_1 = \gamma_2 = 18$ kN/m^3) were used as the reference parameters.

The relationships between the parameters r_ϕ and H/B and the layer factors L_i are depicted in Fig. 3. The influence of r_ϕ is testified by $L_i \leq 1$ in the case of $r_\phi \leq 1$ and by $L_i \geq 1$ when $r_\phi \geq 1$. The influence of r_ϕ decreases when H/B increases. The critical thickness H/B^* is defined as the thickness above which no influence of r_ϕ is noticed ($L_i = 1$).

It is interesting to note that the critical thickness depends on the value of r_ϕ and the considered layer factor L_i with i = c, q, and γ. For instance, in the case of L_c, when $r_\phi = 0.63$ the critical thickness is $H/B^* = 3$ but when $r_\phi = 0.43$ the critical thickness moves to $H/B^* = 6$. When considering the case of $r_\phi = 0.43$, while the critical thickness is $H/B^* = 6$ for L_c, the critical thickness is $H/B^* > 6$ for L_q and the critical thickness is $H/B^* = 3$ for L_γ. This means there is an influence zone delimited by H/B and r_ϕ. The influence zone will be discussed later in this paper.

Eq. (4) below is empirically proposed for the calculation of $L_c^{r_c=1}$, $L_q^{D_f/B=1}$, and $L_\gamma^{r_\gamma=1}$.

$$L_i = a r_\phi{}^5 * e^{b r_\phi} \quad (4)$$

where i = c, q, and γ. The equations of the coefficients a and b are presented in Table 2. Fig. 3 can be used as a design chart.

7. INFLUENCE OF r_ϕ, r_c, D_f, and r_γ ON LAYER FACTORS (DESIGN CHARTS PARTII)

The parameters r_c, D_f and r_γ affect L_c, L_q, and L_γ respectively (See the diagram in Fig. 2). The relationship between L_c, L_q, and L_γ and the couples (r_ϕ and r_c), (r_ϕ and D_f) and (r_ϕ and r_γ) are depicted in Fig. 4 when $H/B = 0.25$.
The layer factor L_q and L_c increase with increasing r_c and r_γ while the layer factor L_q inversely increases with D_f. In Fig. 4, we have (1) $r_c = 1$, $D_f/B = 1$ and $r_\gamma = 1$, and (2) $r_c \neq 1$, $D_f/B \neq 1$ and $r_\gamma \neq 1$. The layer factors obtained with $r_c = 1$, $D_f/B = 1$, and $r_\gamma = 1$ are referred to as $L_c^{r_c=1}$, $L_q^{D_f/B=1}$, and $L_\gamma^{r_\gamma=1}$. On the other side layer factors investigated with $r_c \neq 1$, $D_f/B \neq 1$ and $r_\gamma \neq 1$ are referred to as $L_c^{r_c\neq1}$, $L_q^{D_f/B\neq1}$ and $L_\gamma^{r_\gamma\neq1}$. It is suggested that the influence of r_c, D_f/B and r_γ can be obtained separately by dividing the $L_c^{r_c\neq1}$, $L_q^{D_f/B\neq1}$ and $L_\gamma^{r_\gamma\neq1}$ by $L_c^{r_c=1}$, $L_q^{D_f/B=1}$ and $L_\gamma^{r_\gamma=1}$ respectively. New influence factors ξ_c, ξ_q, and ξ_γ are defined as follows: $\xi_c = L_c^{r_c\neq1}/L_c^{r_c=1}$, $\xi_q = L_q^{D_f/B\neq1}/L_q^{D_f/B=1}$, and $\xi_\gamma = L_\gamma^{r_\gamma\neq1}/L_\gamma^{r_\gamma=1}$.

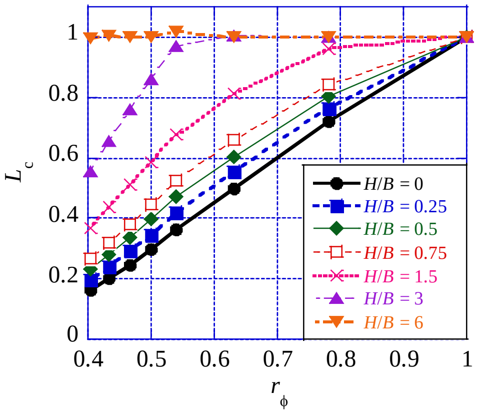

(a) L_c in case of $r_\phi \leq 1$

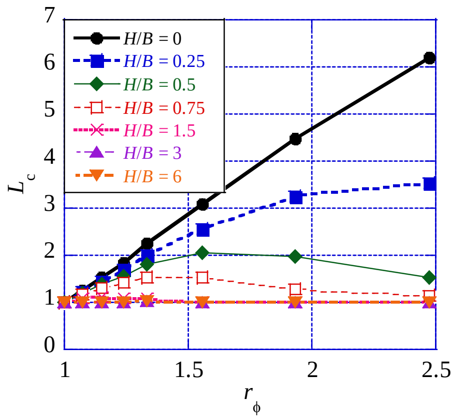

(b) L_c in case of $r_\phi \geq 1$

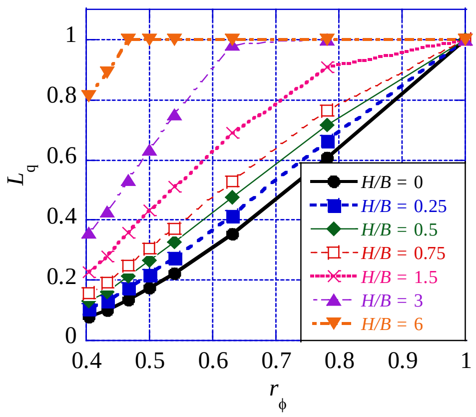

(c) L_q in case of $r_\phi \leq 1$

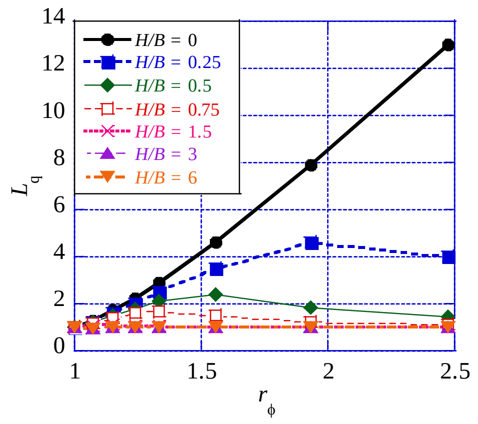

(d) L_q in case of $r_\phi \geq 1$

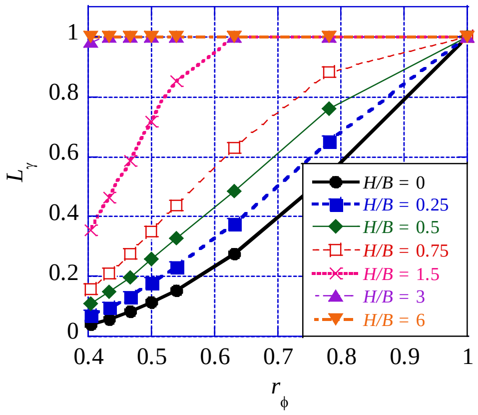

(e) L_γ in case of $r_\phi \leq 1$

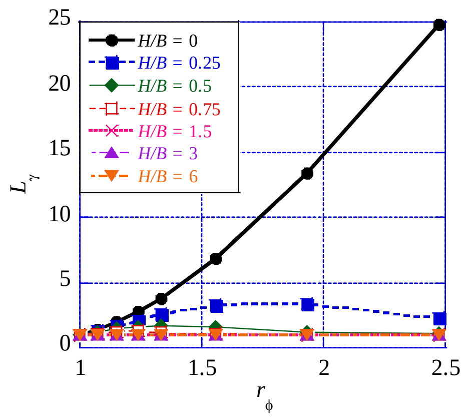

(f) L_γ in case of $r_\phi \geq 1$

Fig. 3 Influence of r_ϕ and H/B on L_i with i = c, q, γ

Table 2 The coefficients a, and b in Eq. (4)

		$r_\phi > 1$	$r_\phi < 1$
$L_c^{r_c=1}$	a	$6.8844(H/B)^2 + 18.816(H/B) + 5.2077$	$37.382(H/B)^2 + 120.64(H/B) + 83.829$
	b	$-1.8311(H/B) - 1.805$	$-0.7561(H/B) - 4.6249$
$L_q^{D_f=1B}$	a	$-14.801(H/B)^2 + 43.29(H/B) + 3.524$	$27.121(H/B)^2 + 48.234(H/B) + 36.29$
	b	$-2.5162(H/B) - 1.5009$	$-0.6386(H/B) - 3.8634$
$L_\gamma^{r_\gamma=1}$	a	$-77.799(H/B)^2 + 86.43(H/B) + 3.4669$	$217.15(H/B)^2 - 12.096(H/B) + 18.076$
	b	$-2.8904(H/B) - 1.4771$	$-2.3144(H/B) - 2.9041$

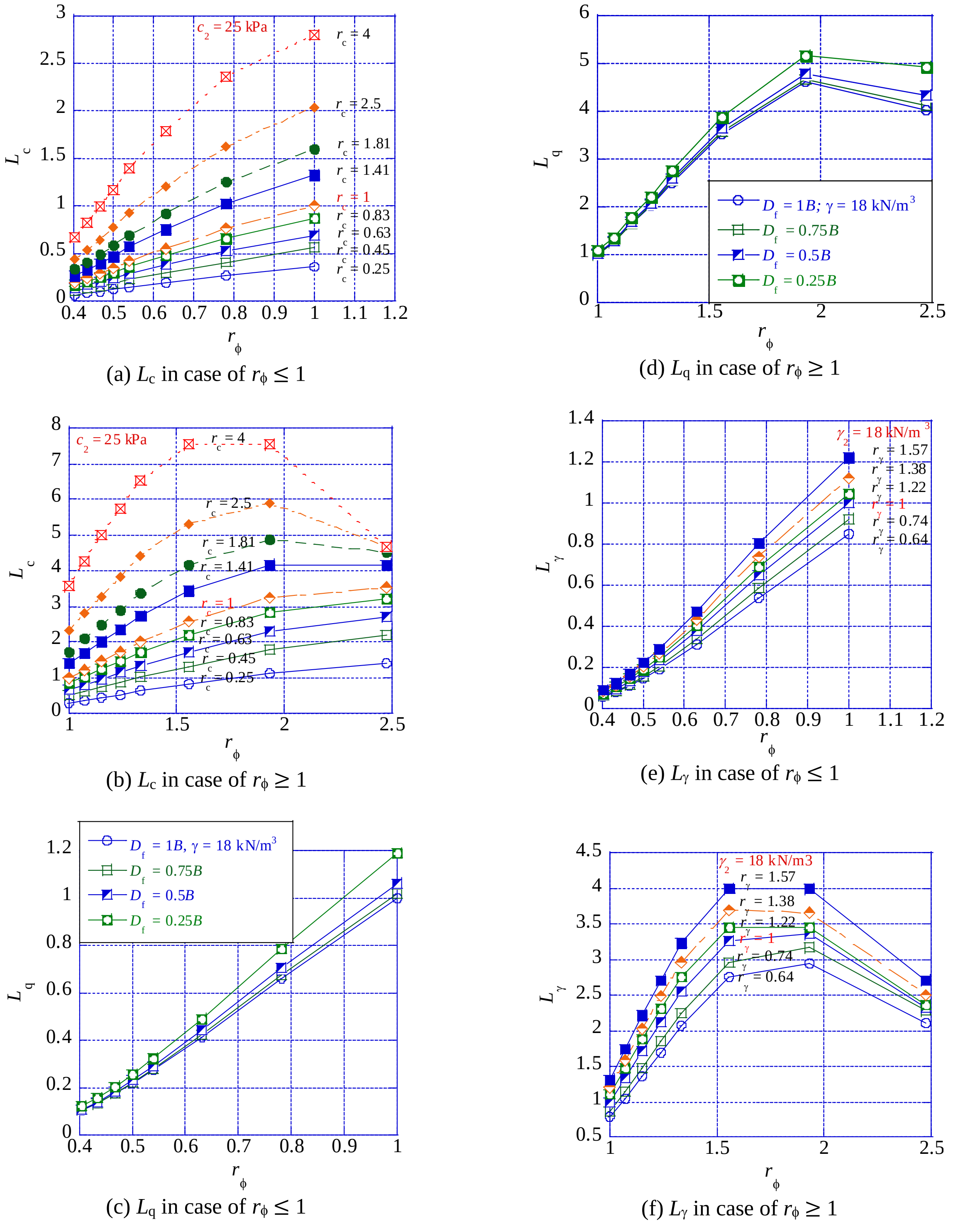

(a) L_c in case of $r_\phi \leq 1$

(d) L_q in case of $r_\phi \geq 1$

(b) L_c in case of $r_\phi \geq 1$

(e) L_γ in case of $r_\phi \leq 1$

(c) L_q in case of $r_\phi \leq 1$

(f) L_γ in case of $r_\phi \geq 1$

Fig. 4 Influence of couples (r_ϕ and r_c), (r_ϕ and D_f) and (r_ϕ and r_γ) on L_c, L_q and L_γ respectively, ($H/B = 0.25$)

The layer factors can therefore be expressed with the formulas in Eq. (5), Eq. (6), and Eq. (7) below.

$$L_c = \xi_c L_c^{r_c=1} \tag{5}$$

$$L_q = \xi_q L_q^{D_f/B=1} \tag{6}$$

$$L_\gamma = \xi_\gamma L_\gamma^{r_\gamma=1} \tag{7}$$

where ξ_c, ξ_q, and ξ_γ stand as the influences of r_c, D_f, and r_γ respectively. $L_c^{r_c=1}$, $L_q^{D_f/B=1}$ and $L_\gamma^{r_\gamma=1}$ are the influences of r_ϕ.

The bearing capacity formula is then expressed by Eq. (8) below.

In Eq. (8), N_c, N_q, and N_g are obtained using ϕ_1 in the traditional methods.

$$q_{\mathrm{ult}} = c_1 N_c L_c + q N_q L_q + 0.5\gamma_1 B N_\gamma L_\gamma \quad (8)$$

Where $\boldsymbol{c_1}$ = cohesion of the top layer; q = overburden pressure; γ_1 = unit weight of the top layer; N_c, N_q, and N_γ = bearing capacity factors obtained using frictional angle ϕ_1 of the top layer in the traditional methods, B = footing width and L_c, L_q and, L_γ are Layer factors defined in Eq. (5)-(7).

Variations of ξ_c, ξ_q, and ξ_γ are depicted in Fig. 5, Fig. 6, and Fig. 7 respectively, for different values of H/B. From Fig. 5(a) and (e), Fig. 6(a) and (e), and Fig. 7(a) and (e) it is clear that the value of the c_2 (or c_1), γ_2 (or γ_1) and the weight of the surcharge soil (γ) do not have influence, only the value of the ratio r_c, r_γ , and D_f are important.

The behavior of ξ_c and ξ_γ are similar, ξ_c (ξ_γ) increases when r_c (r_γ) increases. When r_c (r_γ) > 1 the value of ξ_c (ξ_γ) decreases with the increasing H/B while for r_c (r_γ) < 1 the inverse is observed.

The factor ξ_q inversely increases with D_f. For $r_\phi <$ 1, ξ_q decreases with increasing r_ϕ but increases with increasing H/B, however when $r_\phi > 1$, the inverse is observed.

The curves in Fig. 5, Fig. 6, and Fig. 7 can be used as design charts for the estimation of ξ_c, ξ_q, and ξ_γ in Eq. (5)-(7).

8. FAILURE PATTERNS

Some failure patterns are selectively presented in Fig. 8, while the black line indicates the border between the two soil layers. The norm of the strain rate is represented by contour lines in the range of $\dot{e}_{\min}$ (=0) ~ $\dot{e}_{\max}$. By attributing to each soil layer its strength parameters, RPFEM has shown that the bottom layer may lead to punching failure in the case of a softer bottom while in the case of a stiffer bottom layer, it may lead to local failure. These effects of the bottom layer cannot be obtained with the average strength parameters suggested by the previous studies. Three types of failure modes are observed in each case of r_ϕ ($r_\phi \leq 1$ and $r_\phi \geq 1$). In the case of $r_\phi \leq 1$, general shear failure, transitional shear failure, and punching shear failure are observed. In the case of $r_\phi \geq 1$, a general shear failure, a transitional shear failure, and a local shear failure are obtained. A series of 592 cases of bearing capacity was performed to identify under which conditions each type of failure occurs. The conditions necessary for each failure type are presented in Fig. 9 along with the line of the critical thickness of the top layer.

9. MERIT OF THE USED METHOD AND VALIDATION OF THE PROPOSED EQUATION

Fig. 10 compares the theories in Table 1 with RPFEM using soil characteristics from Table 3 (B = 1m, D_f = 1B). In softer bottom layers, RPFEM generally agrees with [33] and [31] but differs from [34] in certain scenarios. Notably, RPFEM shows constant bearing capacity beyond H/B = 3, challenging Bowles' assumptions about critical thickness, $d = B/2 \tan(45+\phi_1/2) = 0.88$. In stiffer bottom layers, RPFEM aligns with [34] but differs from [33] and [31] in critical thickness values.

To address discrepancies in Fig. 10, Fig. 11 depicts failure patterns at H/B = 0.75. RPFEM shows a punching shear failure with a softer bottom layer (Fig. 11(a)), contrasting with general shear failures in [34] and [31]. RPFEM's punch through the top layer contributes to lower bearing capacity, evident in Fig. 10(a). Good agreement with [33] is attributed to using specific strength parameters from that source.

In Fig. 11(b), [31]'s wider shear band justifies its higher bearing capacity in Fig. 10(b). RPFEM's localized failure reflects the stiffer bottom layer's effect. Differences with [33] arise from distinct soil characteristics. RPFEM, attributing specific strength parameters to each layer, highlights bottom-layer effects not captured by average parameters in previous studies.

[21] conducted a study on the bearing capacity of circular footing on a weak sand layer overlying a dense sand deposit. They introduced a bearing capacity ratio (BCR), defined as the ratio of the footing's bearing capacity on layered sand to that on homogeneous sand with a friction angle ϕ_2 for the bottom layer. The BCR calculated using Eq. (8), were compared with those of [21] for three cases.

For case1 (ϕ_1 = 30 deg., γ_1 = 13.5 kN/m³; ϕ_2 = 40 deg., γ_2 = 17.5 kN/m³), corresponding to (r_ϕ = 1.67; r_γ = 1.3) for Eq. (8). For case2 (ϕ_1 = 36 deg., γ_1 = 16 kN/m³; ϕ_2 = 40 deg., γ_2 = 17.5 kN/m³), the ratios are (r_ϕ = 1.15; r_γ = 1.09). Finally, for case3 (ϕ_1 = 36 deg., γ_1 = 16 kN/m³; ϕ_2 = 44 deg., γ_2 = 19 kN/m³), the ratios are (r_ϕ = 1.33; r_γ = 1.19).

The comparison results, illustrated in Fig. 12, reveal an overall good agreement, affirming the capability of the proposed equation to accurately estimate the bearing capacity.

Table 3. Strength parameters of soils used for comparison

	ϕ (degrees)	c (kPa)	γ (kN / m^3)
Soil 1 (Bowles 1996) [34]	20	20	17.3
Soil 2, (Typical Sandy loam)	35	10	15
Soil 3, Clayey sand (Azam and Wang 1991) [33]	31	9.17	16.56

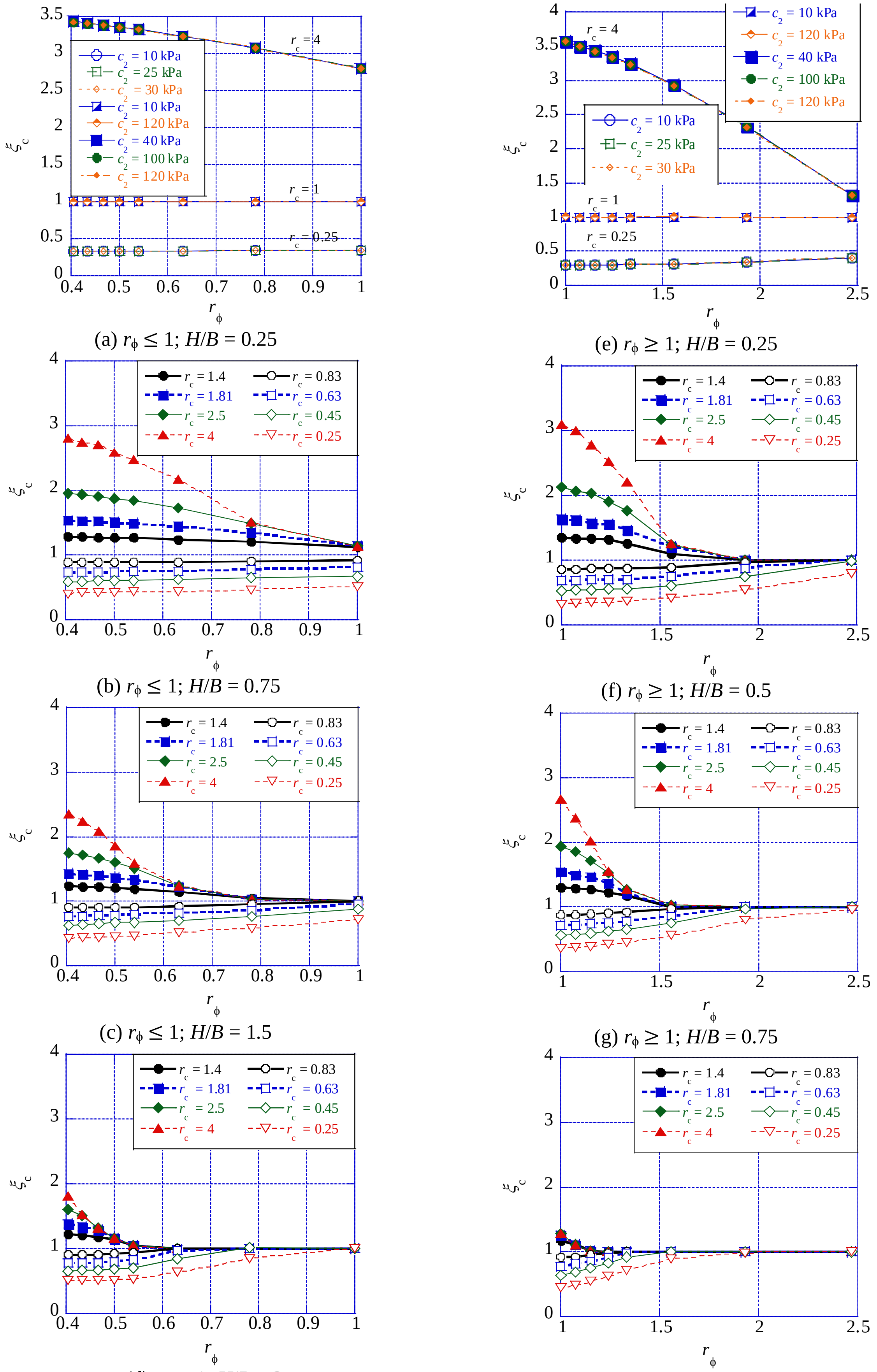

(a) $r_\phi \leq 1$; H/B = 0.25

(e) $r_\phi \geq 1$; H/B = 0.25

(b) $r_\phi \leq 1$; H/B = 0.75

(f) $r_\phi \geq 1$; H/B = 0.5

(c) $r_\phi \leq 1$; H/B = 1.5

(g) $r_\phi \geq 1$; H/B = 0.75

(d) $r_\phi \leq 1$; H/B = 3

(h) $r_\phi \geq 1$; H/B = 1.5

Fig. 5. Influence of r_c and r_ϕ on ξ_c

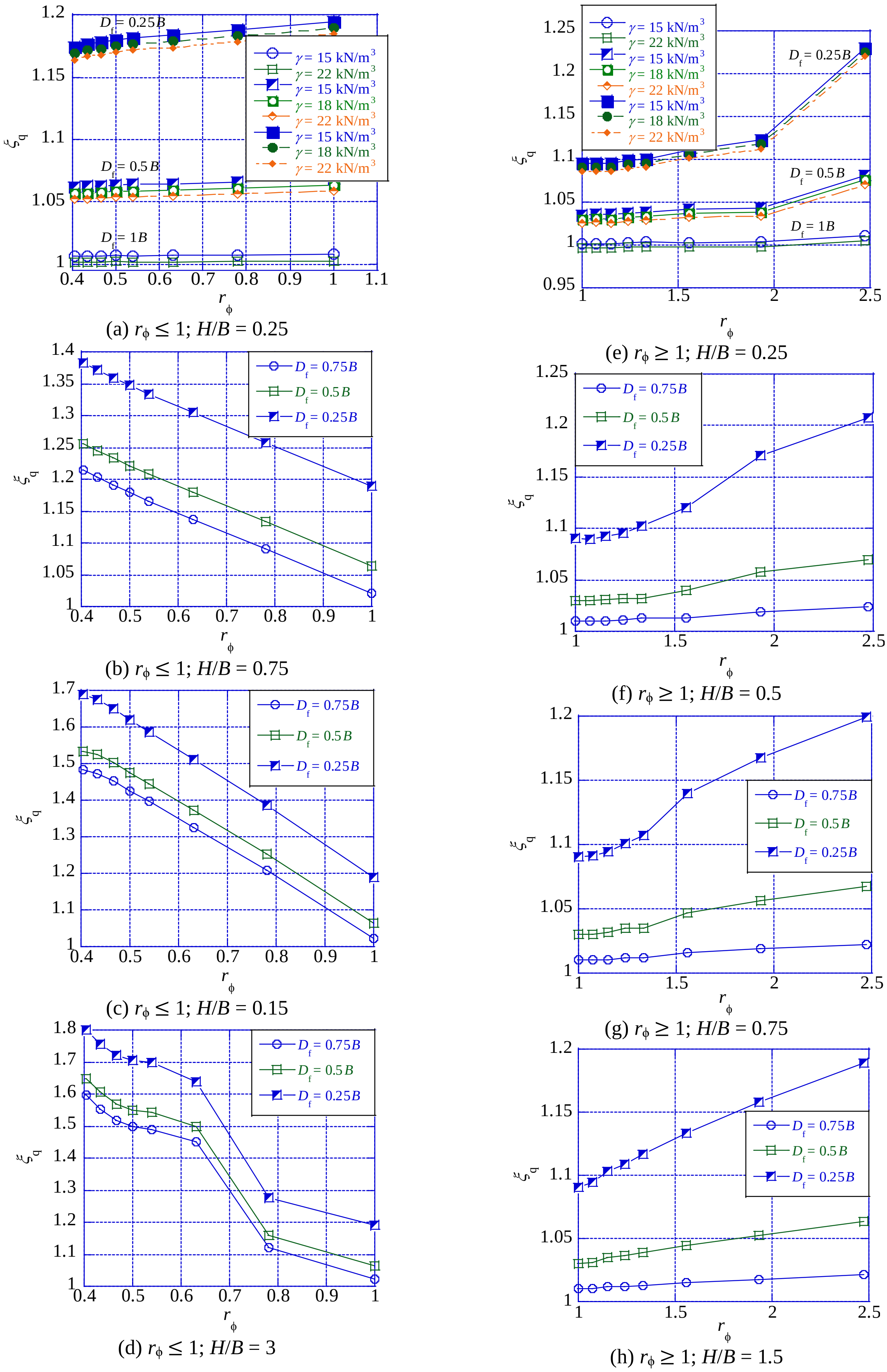

Fig. 6. Influence of D_f and r_ϕ on ξ_q

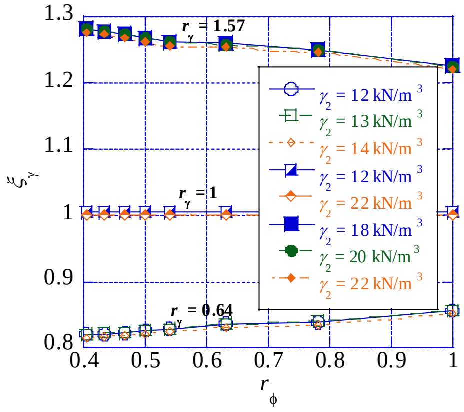

(a) $r_\phi \leq 1$; H/B = 0. 25

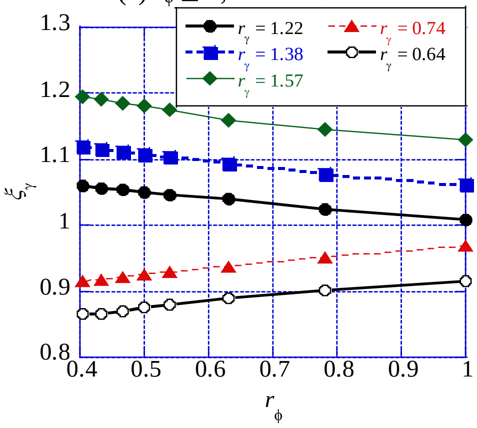

(b) $r_\phi \leq 1$; H/B = 0.5

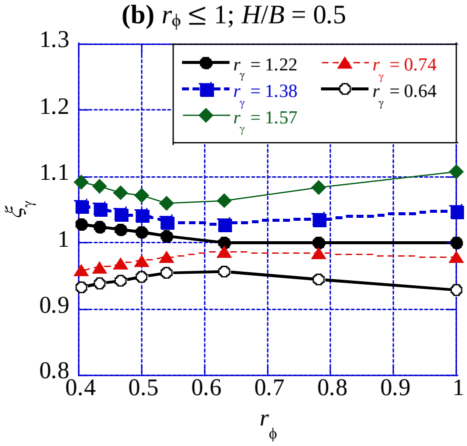

(c) $r_\phi \leq 1$; H/B = 1. 5

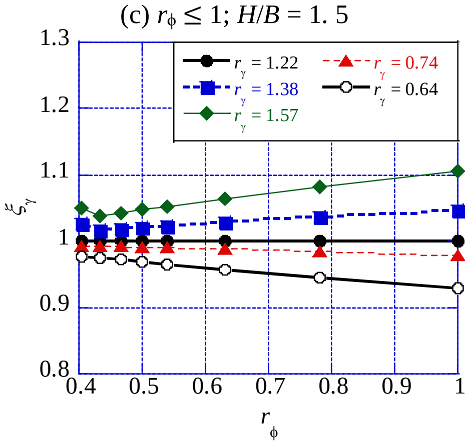

(d) $r_\phi \leq 1$; H/B = 6

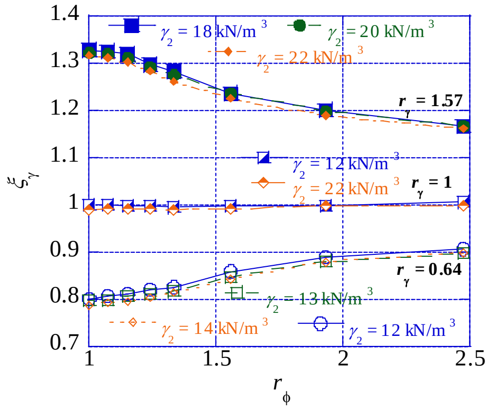

(e) $r_\phi \geq 1$; H/B = 0.25

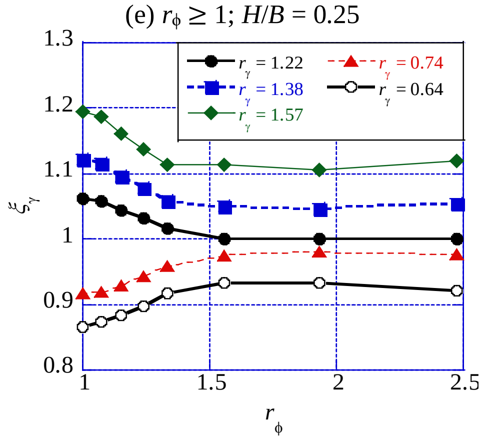

(f) $r_\phi \geq 1$; H/B = 0.5

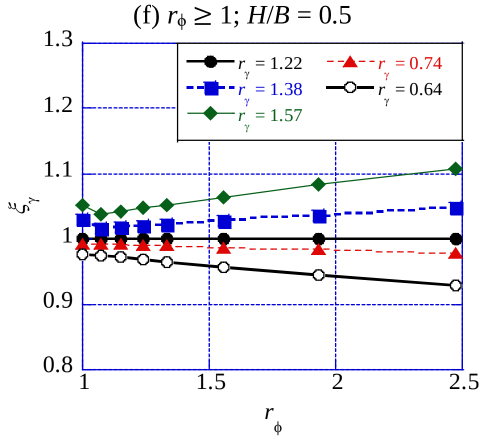

(g) $r_\phi \geq 1$; H/B = 1.5

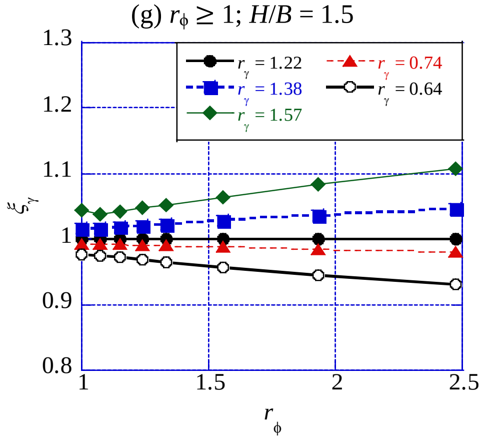

(h) $r_\phi \geq 1$; H/B = 6

Fig. 7. Influence of r_γ and r_ϕ on ξ_γ

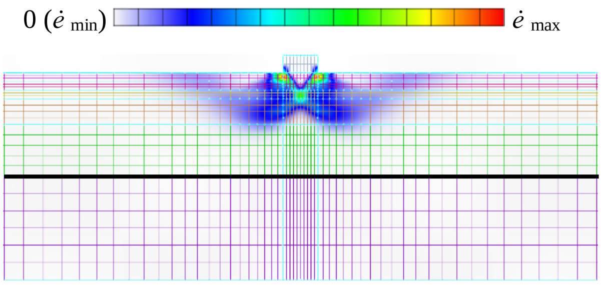

(a) H/B = 3; r_ϕ = 1.93 (General shear failure: Shear planes extend to the surface, without penetrating the bottom layer, without a punch)

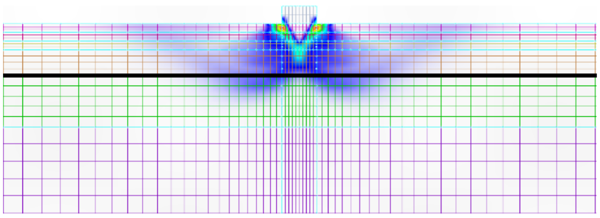

(b) H/B = 1.5, r_ϕ = 0.78 (Transitional shear failure: Like General failure but penetrating the bottom layer)

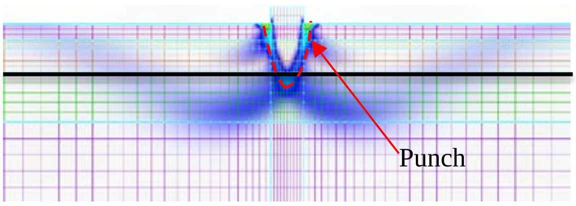

(c) H/B = 1.5, r_ϕ = 0.43 (Punching shear failure: a punch of top soil breaks through the bottom layer)

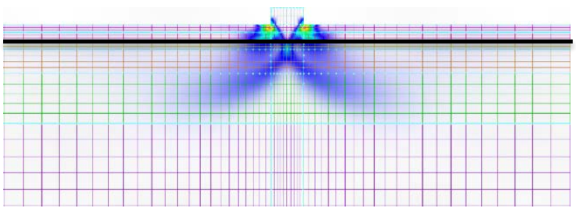

(d) H/B = 0.5, r_ϕ = 1.33 (Local shear failure = the shear planes do not extend to the surface)

Fig. 8 Failure patterns

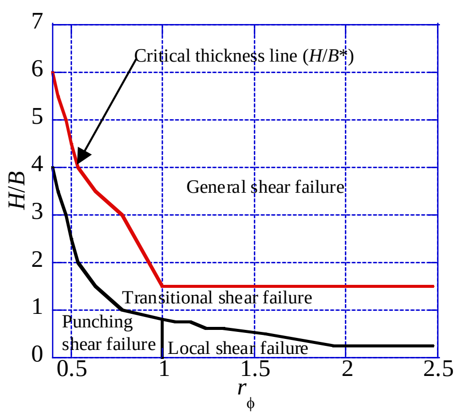

Fig. 9 Failure type as a function of r_ϕ and H/B

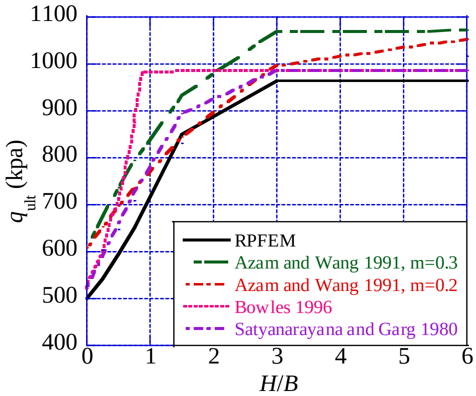

(a) Softer Bottom layer (Soil 1 under Soil 3)

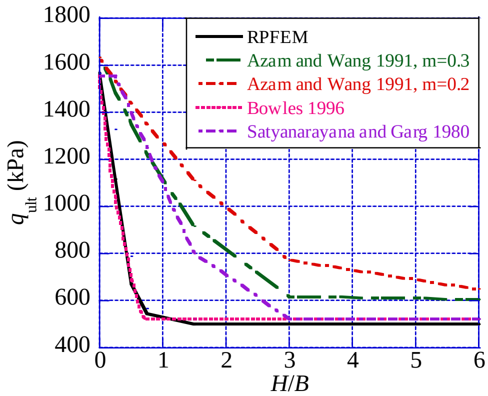

(b) Stiffer Bottom layer (Soil 2 under Soil 1)

Fig. 10. Comparison of RPFEM with existing theories on bearing capacity of two-layered c-ϕ soils

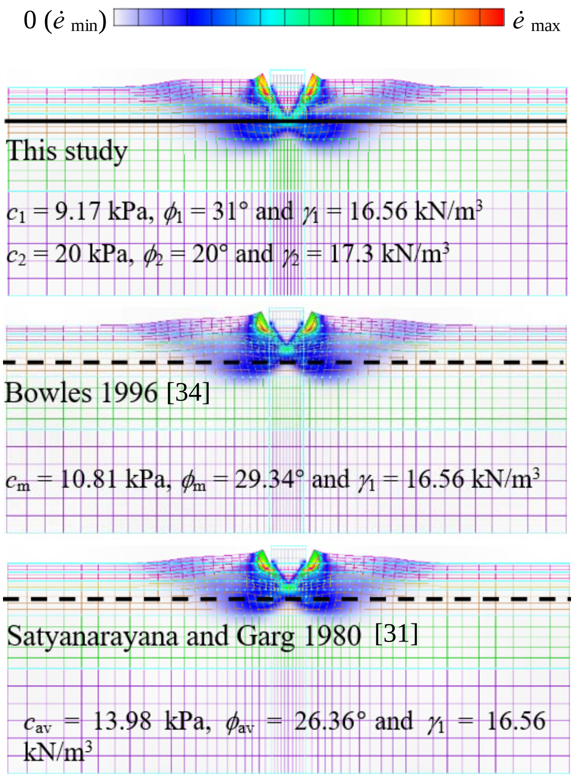

(a) Softer Bottom layer (soil 1 under soil 3)

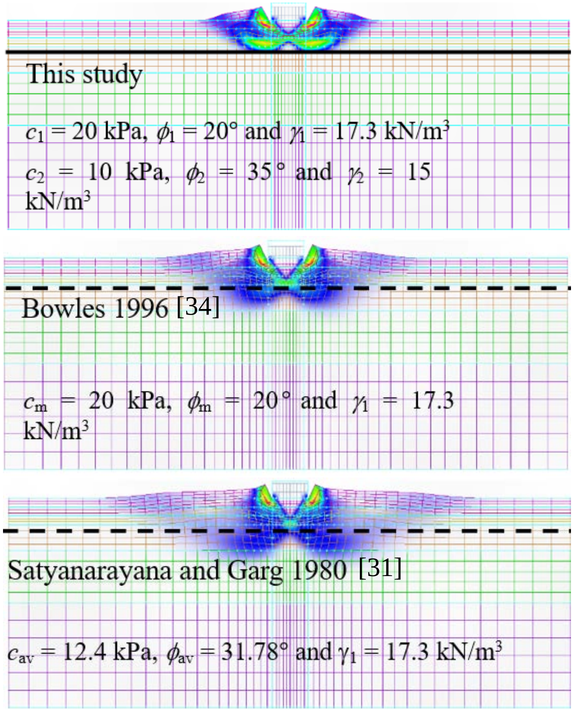

(b) Stiffer Bottom layer (soil 2 under soil 1)

Fig. 11. Comparison of failure patterns (H/B = 0.75)

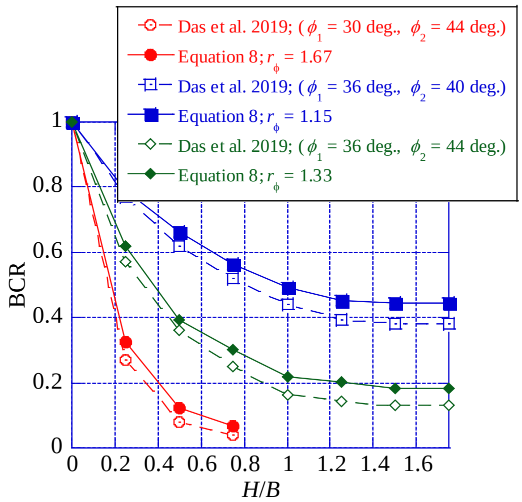

Fig. 12 Validation of Equation (8)

10. CONCLUSIONS

This study's specific strength parameters for each soil layer reveal punching failure with a softer bottom layer and local failure with a stiffer bottom layer, not captured by prior average parameter approaches.

The failure type depends on r_ϕ and H/B values. A proposed chart summarizes conditions for different failure types in two-layered c-ϕ soil bearing capacity evaluation. The critical thickness H/B^* is not as suggested by prior studies; it's a function of r_ϕ.

Introducing layer factors (L_c, L_q, L_γ) to account for the bottom layer's effect, a new formula for two-layered c-ϕ soil bearing capacity is proposed and validated against existing theories, providing a more nuanced understanding of varying soil conditions.

11. REFERENCES

[1] Meyerhof G. G., Ultimate bearing capacity of footings on sand layer overlying clay. Can Geotech J., 11(2), 1974, pp. 223–229.

[2] Kenny M. J. and Andrawes K. Z., The bearing capacity of footings on a sand layer overlying soft clay. Geotechnique, 47(2), 1979, pp. 339-345.

[3] Hanna A. M. and Meyerhof G. G., Design charts for ultimate bearing capacity of foundations on sand overlying soft clay. Can Geotech J., 17(2), 1980, pp. 300-303.

[4] Griffiths D. V., Computation of bearing capacity on layered soils. In Proc., 4th int. conf., Num. meth. Geomech., 1982, pp. 163-170.

[5] Das B. M. and Dallo K. F., Bearing capacity of shallow foundations on a strong sand layer underlain by soft clay. Civ Eng Pract Des Eng., 3(5), 1984, pp. 417-438.

[6] Michalowski R. L. and Shi L., Bearing capacity of footings over 2-layer foundation soils. J Geotech Eng., 21(5), 1995, pp. 421– 428.

[7] Burd H. J. and Frydman S., Bearing capacity of plane-strain footings on layered soils. Can Geotech J., 34(2), 1997, pp. 241-253.

[8] Okamura M., Takemura J., and Kimura T., Bearing capacity predictions on sand overlying clay based on limit equilibrium methods. Soils Found., 38(1), 1998, pp. 181–194.

[9] Shiau J. S., Lyamin A. V., and Sloan S. W., Bearing capacity of sand layer on clay by finite element limit analysis. Can Geotech J., 40(5), 2003, pp. 900–915.

[10] Qin H. L., and Huang M.S., Upper- bound method for calculating bearing capacity of strip footings on two-layer soils. Chinese J Geotech Eng., 30(4), 2008, pp. 611-616.

[11] Huang M. and Qin H. L., Upper-bound multi-rigid-block solutions for bearing capacity of two-layered soils. Comput Geotech., 36(3), 2009, pp. 52-59.

[12] Salimi E. S., Abbo A. J., and Kouretzis G., Bearing capacity of strip footings on sand over clay. Can Geotech J., 56(5), 2019, pp. 699-709. https://doi.org/10.1139/cgj-2017-0489.

[13] Button S. J., The Bearing Capacity of Footings on a Two-Layer Cohesive Subsoil. 3rd ICSMFE, Vol. 1, 1953, pp. 332-335.

[14] Meyerhof G. G. and Hanna A.M., Ultimate

bearing capacity of foundations on layered soils under inclined load. Can Geotech J., 15(4), 1978, pp. 565–572.

[15] Siva R. A. and Srinivasan R. J., Bearing capacity of footings on layered clays. J Soil Mech Found Division, ASCE, 938M2, 1967, pp. 83-99.

[16] Brown J. and Meyerhof G. G., Experimental study of bearing capacity in layered clays. In Proc. Stmenth Int. Con. Soil Mech. Found. Eng., (2), 1969, pp. 45-51.

[17] Desai C. S. and Reese L., Ultimate capacity of circular footings on layered soils. J Indian Nat. Soc. Soil Mech. Found. Eng., 96(1), 1970a., pp. 41-50.

[18] Desai C. S. and Reese L., Analysis of circular footings on layered soils. J Soil Mech. Found. Division, ASCE., 96(4), 1970b, pp. 1289-1310.

[19] Merlfleld R. S., Sloan S. W., and Yu H. S., Rigorous plasticity solutions for the bearing capacity of two-layered clays. Geotechnique, 49(4), 1999, pp. 471-490.

[20] Yao X., Minghua Z., and Heng Z., Undrained stability of strip footing above voids in two-layered clays by finite element limit analysis. Comput Geotech., 97, 2018, pp. 124–133.

[21] Das P. P., Khatri V. N., and Dutta R. K., Bearing capacity of ring footing on weak sand layer overlying a dense sand deposit. Geomechanics and Geoengineering, Vol. 16, Issue 4, 2019, pp. 249-262.DOI: 10.1080/17486025.2019.1664775.

[22] Hanna A. M., Foundations on strong sand overlying weak sand. J Geotech Eng Division, ASCE, 107(7), 1981, pp. 915-927.

[23] Hanna A. M., Bearing capacity of foundations on a weak sand layer overlying a strong deposit. Can Geotech J., 19(3), 1982, pp. 392-396.

[24] Das B. M. and Munoz R. F., Bearing capacity of eccentrically loaded continuous foundations on layered sand. Transp Res Rec., 1984, P.28-31.

[25] Farah C. A., Ultimate bearing capacity of Shallow foundations on layered soils. MSc thesis, Civil and Environmental Engineering, Concordia Univ, 2004; Quebec.

[26] Kumar A., Ohri M. L., and Bansal R. K., Bearing capacity tests of strip footings on reinforced layered soil. Geotech Geol Eng., 25(2), 2007, pp. 139-150.

[27] Mabrouki A., Benmeddour D., and Frank R, Numerical study of the bearing capacity for two interfering strip footings on sands. Comput Geotech., 37(4), 2010, pp. 431–439.

[28] Khatri V., Kumar J., and Akhtar S., Bearing capacity of foundations with inclusion of dense sand layer over loose sand strata. Int J Geomech., 17(10), 2017, pp. 06017018.

[29] Salimi E. S., Abbo A. J., and Kouretzis G., Bearing capacity of strip footings on layered sands. Comput Geotech., 114(2), 2019, pp. 103-101.

[30] Purushothamaraj P., Ramiah B. K., and Venkatakrishna Rao K. N., Bearing capacity of strip footing in two-layered cohesive-friction soils. Can Geotech J., 11(1), 1974, pp. 32-45.

[31] Satyanarayana A. M. and Garg R.K. "Bearing capacity of footings on layered c-φ soils". J. Geotech. Eng. Div., ASCE, 106 (7), 1980, pp. 819–824.

[32] Florkiewicz A., Upper bound to bearing capacity of layered soils. Can Geotech J, 26(4), 1989, pp. 730-736.

[33] Azam G. and Wang M.C., Bearing Capacity of Strip Footing Supported by Two-layer c-φ Soils. Washington, D. C: Transportation Research Record, Transportation Research Board No. 1331, 1991, pp. 56–66.

[34] Bowles J. E., Foundations Analysis and Design. McGraw-Hill Publishing Company, New York, 1996, pp.1-1023.

[35] Tamura T., Kobayashi S., and Sumi T. Limit analysis of soil structure by rigid plastic finite element method. Soils Found., 24(1), 1984, pp. 34-42.

[36] Tamura T., Kobayashi S., and Sumi T., Rigid plastic finite element method for frictional soil. Soils and Found., 27(3), 1987, pp. 1-12.

[37] Du N.L., Ohtsuka S., Hoshina T., and Isobe K., Discussion on size effect of footing in ultimate bearing capacity of sandy soil using rigid plastic finite element method. Soils and Found., 56(1), 2016, pp. 93-103.

[38] Hoshina T., Ohtsuka S., and Isobe K. Ultimate bearing capacity of ground by rigid plastic finite element method taking account of stress-dependent non-linear strength property. J. Appl. Mech., 6, 2011, pp. 191–200 (in Japanese).

[39] Terzaghi K., Theoretical Soil Mechanics. Chapman and Hall, London, 1943, pp. 1- 510.